Numerical study of the *glass–glass* transition in short-ranged attractive colloids

2004 J. Phys.: Condens. Matter 16 S4849

(http://iopscience.iop.org/0953-8984/16/42/004)

INSTITUTE OF PHYSICS PUBLISHING JOURNAL OF PHYSICS: CONDENSED MATTER

J. Phys.: Condens. Matter **16** (2004) S4849–S4860 PII: S0953-8984(04)78618-X

Numerical study of the *glass–glass* transition in short-ranged attractive colloids

Emanuela Zaccarelli[1], **Francesco Sciortino**[1,2] **and Piero Tartaglia**[1,3]

[1] Dipartimento di Fisica, Università di Roma La Sapienza, Piazzale Aldo Moro 5, I-00185 Rome, Italy
[2] INFM-CRS SOFT, Università di Roma La Sapienza, Piazza Aldo Moro 2, I-00185 Roma, Italy
[3] INFM-CRS SMC, Università di Roma La Sapienza, Piazza Aldo Moro 2, I-00185 Roma, Italy

E-mail: emanuela.zaccarelli@phys.uniroma1.it

Received 30 March 2004
Published 8 October 2004
Online at stacks.iop.org/JPhysCM/16/S4849
doi:10.1088/0953-8984/16/42/004

Abstract

We report extensive numerical simulations in the *glass* region for a simple model of short-ranged attractive colloids, the square well model. We investigate the behaviour of the density autocorrelation function and of the static structure factor in the region of temperatures and packing fractions where a glass–glass transition is expected according to theoretical predictions. We strengthen our observations by studying both waiting time and history dependence of the numerical results. We provide evidence supporting the possibility that activated bond-breaking processes destabilize the attractive glass, preventing the full observation of a sharp glass–glass kinetic transition.

1. Introduction

The combination of theory [1–7], experiments [8–12] and numerical simulations [13–18] for short-ranged attractive colloidal systems, i.e. colloid–polymer mixtures in which the size of the polymers is only a few per cent of that of the colloidal particles, has led in the last few years to clear evidence of anomalous dynamical properties for dense colloidal systems. In particular, the existence of a re-entrant region of (super-cooled) liquid state, which is stable up to packing fractions higher than the correspondent purely repulsive system (hard spheres), has been established. From this liquid region one can approach dynamical arrest in two distinct ways [19], depending on which control parameters for the system are manipulated. Thus, an increase of colloid density leads to the well known hard-sphere (or simply 'repulsive') glass, while a stronger attraction, which is experimentally realized via an increase of polymer concentration, produces the so-called attractive glass, where colloidal particles are stabilized by 'bonding'. Moreover, an efficient competition between these two mechanisms of arrest originates a peculiar behaviour of dynamical correlation functions within the re-entrant fluid

region, in particular a logarithmic decay for the density autocorrelation functions and a sub-diffusive regime for the mean squared particle displacement [15, 16, 20, 27]. All these features were first predicted by the mode coupling theory (MCT) [21] on the basis of the existence in the control parameter space for these systems of a higher order singularity in the solutions of MCT equations, which entirely governs the anomalous dynamics. This particular point in the phase diagram, named the A_4 singularity, is found for a particular value of the three control parameters, i.e. temperature, volume fraction of the colloids and range of the attractive interaction, where the liquid, the attractive glass and the hard-sphere glass solutions all merge into a single point. The key parameter for the existence of such a point is the attractive range of the potential Δ (experimentally set by the ratio of polymer gyration radius to the colloidal radius): for $\Delta > \Delta^*$ there is no distinction between the two glassy states, while for $\Delta < \Delta^*$ there exists a discontinuous glass–glass transition between the two [3, 4]. The glass–glass transition terminates at an end-point, named A_3, beyond which the two glasses are indistinguishable. Such a kinetic glass–glass transition is one of the most difficult MCT predictions to detect, due to the fact that it lies entirely in a non-equilibrium region where both experiments and simulations are highly non-trivial.

On the other hand, while there is convincing evidence, also for molecular glass-formers, of the accuracy of MCT predictions in the liquid regime [22], the same does not apply for regions where the theory predicts a *glass*. Indeed, the MCT glass is commonly termed 'ideal', because it arises without the inclusion of the so-called hopping processes, i.e. further relaxing processes which eventually allow the system to still restore ergodicity, beyond the ideal MCT transition [23]. This may be better explained in the free energy landscape picture, where a glassy state is represented as a local (metastable) minimum and a hopping process corresponds to a jump between different minima, via a low order saddle-point [24].

In this paper, we report an extensive numerical study of the glass–glass transition for a specific simple model [15], for which the locations of the MCT transition lines and of the higher order singularity have been extensively studied and estimated via a mapping procedure [16, 27]. Thereby, after explaining in detail how this mapping is performed, we report results in the glassy region, including static and dynamical properties of the glassy states, as well as comparing results obtained following different histories for the system, due to their non-equilibrium nature. This will confirm the importance of hopping processes in some mechanisms of glassification, and provide more insight into the MCT applicability to describe different mechanism of arrest. A short account of the main results was already anticipated in a recent letter [29].

2. Methods

We perform event-driven molecular dynamics simulations for a binary mixture of particles interacting via a narrow square-well (SW) potential. The parameters of the mixture are chosen in order to avoid crystallization in the system. Thus, we consider a 50:50 mixture of 700 particles of mass m with diameters $\sigma_{AA} = 1.2$ and $\sigma_{BB} = 1$; the hard-core diameter for the AB interaction is $\sigma_{AB} = (\sigma_{AA} + \sigma_{BB})/2$. We fix the width of the attractive well as $\Delta_{ij}/(\sigma_{ij} + \Delta_{ij}) = 3\%$. Temperature is measured in units of the well-depth u_0, while time units are $\sigma_{BB}(m/u_0)^{1/2}$.

This system was extensively studied previously by means of theory (MCT) and simulations. The combination of both tools allowed us to determine, within some approximations, the location of the MCT lines, and consequently of MCT higher order singularities, for this particular system. In this way, we obtain the best possible diagram for studying the dynamics of the system near the A_4 singularity [16] and crossing the glass–glass transition [29].

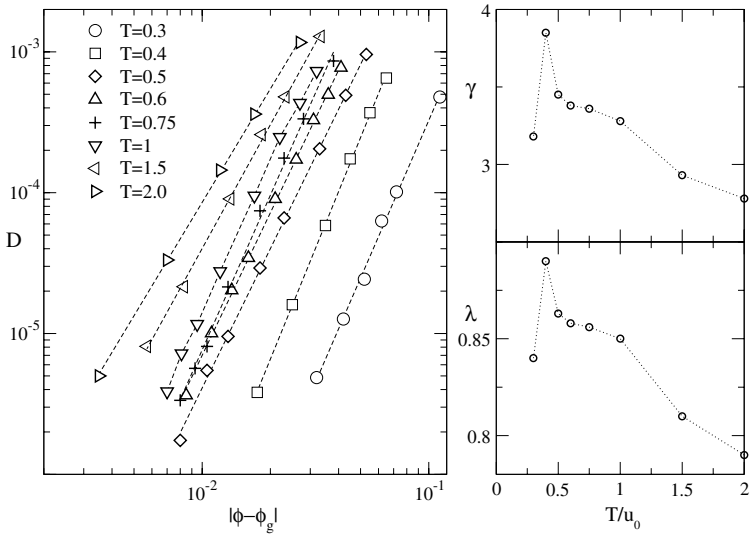

Figure 1. Left-hand panel: diffusion coefficients in the liquid region for various studied temperatures. Dashed lines are power-law fits, with parameters ϕ_g, i.e. the glass transition packing fraction at which $D = 0$, and the exponent γ. Right-hand panel: behaviour of γ, and of the exponent parameter λ, with temperature.

Here, we briefly review how this mapping procedure between theory and simulations is performed. First, we solved MCT equations for our particular binary mixture using as inputs the partial static structure factors calculated within the Percus–Yevick (PY) approximation [28]. In particular, for the static structure calculations, we solved numerically the Ornstein–Zernike equation on a grid of 20 000 wavevectors, with mesh 0.314 1593, while for the binary MCT equations we used a grid of 2000 wavevectors with the same mesh. By solving the equations for a large range of T–ϕ values, the PY–MCT glass lines have been determined. Next, we calculated the diffusion coefficients from simulations in the liquid region, covering four decades in diffusivity values. A fit of these values according to the power-law $D \sim (\phi - \phi_g(T))^\gamma$ provides estimates for the glass transition packing fraction $\phi_g(T)$ (at which the diffusion coefficient would vanish) for the various isotherms and a characteristic exponent γ, which, according to MCT predictions, should grow near a higher order singularity. Note that γ is related to the exponent parameter λ which becomes exactly equal to unity at the MCT singularities (A_3, A_4). Figure 1 shows the fit of the diffusivity data, together with the parameters γ and λ obtained from them. Errors in these values are given by the errors in the fits[4]. The locus $\phi_g(T)$ provides the best numerical estimate of the glass transition lines. Next we perform a bilinear transformation in the control parameter space (ϕ, T), to superimpose the PY–MCT results for the ideal glass line with the extrapolated results from the simulations, following an idea proposed by Sperl [27]. The resulting transformation is found to be

$$\begin{aligned} \phi_{\rm sim} &\to 1.897\phi_{\rm MCT} - 0.3922; \\ T_{\rm sim} &\to 0.5882T_{\rm MCT} - 0.225. \end{aligned} \tag{1}$$

This transformation provides a tool for comparing theoretical predictions and simulation results. Improvements over such a procedure could be obtained by using the numerical 'exact'

[4] The values of γ reported in [15] are consistently higher than those of figure 1, due to the smaller number of numerical points available there and consequently higher uncertainty in the fits.

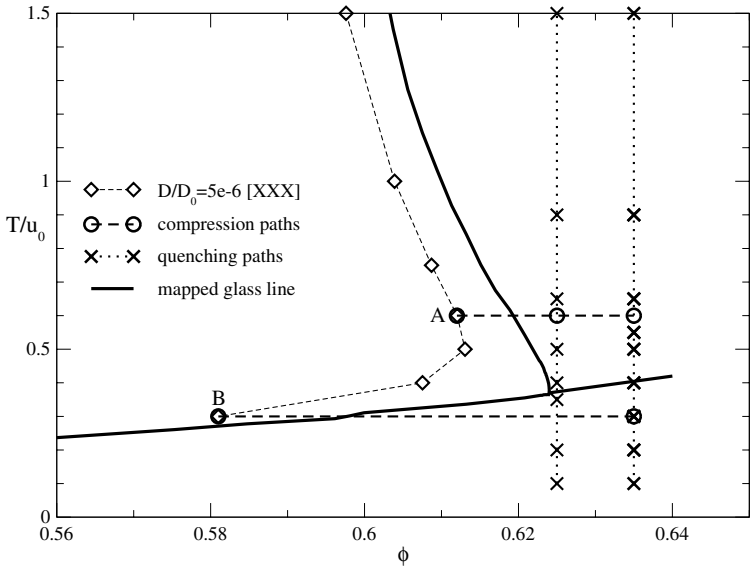

Figure 2. Map of the simulations. We consider two initial state points, labelled A and B, lying along the iso-diffusivity curve (diamond—small dashed curve) calculated in [15], respectively close to the hard-sphere and to the attractive glass transition. We compress these configurations up to two isochores, $\phi = 0.625$ and 0.635, and follow quenches at various temperatures (crosses–dotted lines). The solid curve is the mapped glass line from [16], as described in the text.

structure factors as opposed to the PY closure in the estimate of the ideal MCT lines. Indeed, despite the quite good agreement of the PY solutions, small differences between PY and numerical structure factors are crucial for a full quantitative agreement of theory and simulation results, as recently discussed in [30]. Assuming that the bilinear transformation is invariant for small changes of Δ, we can locate theoretically the position of the A_4 singularity, moving along the Δ-axis in the control parameter space and find the corresponding location for the real system [16]. The qualitative general agreement between predictions and simulation results for the mean squared displacement and density auto-correlation functions shown in [16] strongly supports the validity of the mapping procedure. Having established the quality of the mapping, we can locate the theoretically predicted glass–glass transition for the $\Delta = 0.03$ case which refers to the present simulation parameters. More specifically, the glass–glass line is found to be located in the (ϕ, T)-plane approximately between (0.625, 0.37) and (0.64, 0.41). The resulting liquid–glass and glass–glass lines for the model are shown in figure 2.

Our aim is to perform MD simulations across the glass–glass transition line and study the dynamical properties, in particular the collective density–density correlation functions, both in the hard-sphere and in the attractive glass region. A discontinuity in such properties should be observed, according to MCT, at the glass–glass transition. In order to access the glass region, we used the following procedure, that is schematized in figure 2. We consider the slowest equilibrated liquid state point in the re-entrant region, i.e. corresponding to initial packing fraction and temperature of $\phi_i = 0.612$ and $T_i/u_0 = 0.6$ (labelled as A in the figure). We then rapidly compress the configuration by progressively growing the particle radii in successive steps. In order to investigate the glass–glass transition we choose to compress the system isothermally $\phi = 0.625$ and up to 0.635. At each of the two packing fractions, we then suddenly change the mean square velocities to achieve configurations at several different temperatures (indicated with crosses). A thermostat with a very short characteristic time

kept the temperature constant during the subsequent ageing evolution. This procedure has been repeated for 136 independent initial configurations extracted from the initial equilibrium liquid state.

The system being out of equilibrium, the dynamical observables will also have a dependence on the waiting time t_w, and on the chosen initial state [25, 26]. Thus, in particular, the density autocorrelation functions are defined as

$$\phi_q(t_w + t, t_w) \equiv \langle \rho^*_{\mathbf{q}}(t_w + t)\rho_{\mathbf{q}}(t_w)\rangle / \langle |\rho_{\mathbf{q}}(t_w)|^2\rangle \tag{2}$$

where $\rho_{\mathbf{q}}(t) = \frac{1}{\sqrt{N}} \sum_i e^{i\mathbf{q}\mathbf{r}_i(t)}$ and $\mathbf{r}_i(t)$ are the coordinates of particle i at time t. The correlation functions calculated in this paper always refer to all particles in the mixture. Averages are taken over up to 136 independent initial configurations from the initial liquid state. To assess the problem of a possible path dependence of the results, we also consider a different initial liquid state, this time within the attractive region, i.e. $\phi_i = 0.58$, $T_i/u_0 = 0.3$ (labelled as B in the figure). Moreover, we check that our results are waiting-time independent within a well defined, even though narrow, time window. This has already been discussed in [29]. For the present purposes, we recall that the results reported in this article correspond to $t^*_w = 4 \times 10^3$ which provides sufficient equilibration for the decay processes taking place on a timescale one order of magnitude smaller [26]. For this reason we only show the decay of correlation up to $t = 400$. However, in order to provide convincing evidence that results for $t < 400$ do not depend on the chosen t_w, we will also report results corresponding to a t_w larger by an order of magnitude. Finally, we will discuss the behaviour of static structure factors in the glassy region.

3. Results

Before showing the simulation results, we start by reporting MCT predictions. In figure 3, we show the behaviour of the (total) non-ergodicity factor $f_q = \lim_{t\to\infty} \phi_q(t)$ (where we assume no waiting time dependence), crossing the glass–glass transition along an isochore, at temperatures whose distance from the transition is the same as for the simulated points. It is evident that f_q does not change very much in the hard-sphere glass region, but jumps abruptly at the glass–glass transition, and then changes dramatically with temperature in the attractive region. We want here to draw the reader's attention to the non-monotonic behaviour of f_q in the hard-sphere region with temperature, as this non-trivial feature will also be found in the simulations. The crossing arises because at this isochore at intermediate temperatures (see figure 2) there are two distinct transitions close by, i.e. a standard liquid–glass and a glass–glass one, which can effectively compete. Similarly, if we plot the full time evolution of $\phi_q(t)$ at the same points for a particular wavevector, e.g. at the static structure factor first peak, we find a net difference in the levels of the plateaux reached, i.e. very high for the attractive glasses and much lower for the hard-sphere ones (see figure 2(b) of [29]). We recall here that the glass–glass transition is a purely kinetic phenomenon, which arises from the non-linearity of MCT equations. Thus, there is no abrupt change in the static structure passing from one glass to the other.

Now we turn to the simulation results. We plot the density autocorrelation functions $\phi_q(t, t^*_w)$ for $\phi = 0.625$ at all studied temperatures for the representative wavevector $q\sigma_{BB} \simeq 25$, since their behaviour is similar for all studied wavevectors. The following features are evident in figure 4.

- At higher temperatures, the system is already able to relax to its plateau, even within the small time window studied. Also, the predicted non-monotonic behaviour of the plateau with temperature, found theoretically, is reproduced in full detail.

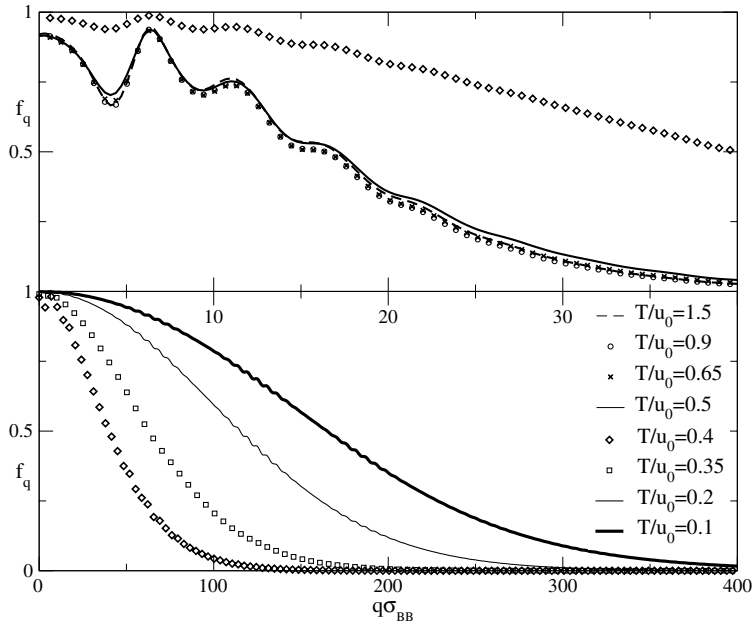

Figure 3. MCT predictions for the number density non-ergodicity parameter f_q for $\phi \simeq 0.5362$ (corresponding to $\phi_{\mathrm{SIM}} = 0.625$). The top one refers to high temperatures, in the hard-sphere glass region, and the bottom one to the lower ones, in the attractive glass. The case $T/u_0 = 0.4$ is reported in both panels. Note the non-monotonicity of f_q in the hard-sphere region, as well as the difference of one order of magnitude in the $q\sigma$ scale betwen the two panels.

- Lowering the temperature, there is a smooth change in the correlators, which start to display a quite evident logarithmic decay, a signature of the higher order MCT singularity that is close by.
- At temperatures already below the glass–glass line, i.e. for $T/u_0 \leqslant 0.4$, the correlators continue quickly to drop, below the expected attractive plateau; a further decrease in temperature elongates the time duration of the plateau, but a decay at longer times is present even in the extreme case $T/u_0 = 0.1$.
- Looking in more detail, we observe that theoretically $f_q(T/u_0 = 0.9) < f_q(T/u_0 = 0.65)$ (see figure 3) while the simulations show the opposite feature at our final time of observation. This may well be due to the inaccuracy of PY structure factors that we used to solve MCT equations [30], or to the fact that hopping processes already start to produce deviations from MCT at $T/u_0 = 0.65$ (in this respect, at the immediately lower temperature $T/u_0 = 0.5$, MCT predictions are very far from the simulation data).

A very similar behaviour is found analysing the different packing fraction $\phi = 0.635$, already reported in [29]. The only difference from the previous case is that no evident crossing of f_q was found there. This is again in agreement with MCT, because the influence of the liquid–glass transition is now less strong, since the chosen isochore lies more deeply into the glassy region.

Conclusions that can be drawn from these results are that the hard-sphere glass predictions are fully reproduced by simulations, while the attractive glass seems to be less stable than predicted. An interpretation of these findings is possible taking into account a relevant parameter for the system at low temperatures, i.e. the lifetime of the attractive bonds. The

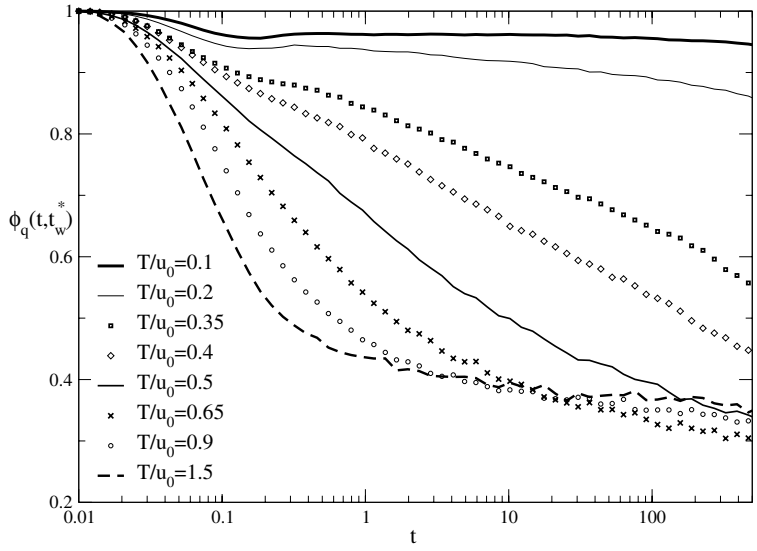

Figure 4. Density correlators calculated from the simulation at $\phi = 0.625$ for $q\sigma_{BB} \simeq 25$ and $t_w^* = 3754$.

square well model is particularly suited to study bond dynamics, since a bond is unambiguously defined when two particles have a pair interaction energy equal to $-u_0$, i.e. they are at a distance less than or equal to Δ. To monitor the dynamical evolution of the bonds, we introduce the 'bond' correlation function $\phi_B(t_w + t, t_w)$, defined as

$$\phi_B(t_w + t, t_w) = \left\langle \sum_{i<j} n_{ij}(t_w) n_{ij}(t_w + t) \right\rangle \Big/ [N n_B(t_w)] \tag{3}$$

where $n_{ij}(t_w)$ is unity if two particles are bonded and zero otherwise, while $n_B(t_w) \equiv \langle \sum_{i<j} n_{ij}(t_w) \rangle / N$ is the average number of bonds per particle at t_w. ϕ_B counts how many of the bonds found at time t_w are still present after time $t_w + t$, independently from any breaking–reforming intermediate process.

The time evolution of $\phi_B(t_w + t, t_w)$, shown in figure 5, is very similar to the one of $\phi_q(t_w + t, t_w)$, suggesting that the decay of density–density correlation is associated with the dynamics of bond breaking. The reason why the shape of the correlators in figure 5 looks similar to density correlators even for high temperatures lies in the fact that we have also taken into account bonds re-forming, once they are broken. Indeed, the packing fraction we are studying ($\phi = 0.635$) is well above the glass transition packing fraction ($\phi_g \sim 0.58$) for simple hard spheres, thus particles are confined to rattle in their cages, and bonds are continuously broken and reformed. To give convincing evidence of the different dynamics taking place at high and low temperatures, we report in figure 6 the bond correlation function, at the two extreme temperatures $T/u_0 = 0.1$ and 1.5, defined above, as well as the same functions but where $n_{ij}(t_w)$ is set to zero at the time when the ij bond is broken, and kept to zero from then on, irrespective of the presence of the ij bond at later times. In the high temperature case, the bond correlation function goes almost to zero when broken bonds are not re-counted, while at low temperature there is no substantial change. In our previous work [29], we have already put forward the observation of relevance of bond dynamics for attractive glasses, by showing how a characteristic type of hopping process takes place in the attractive glass, pre-empting the observation of a sharp glass–glass transition, as predicted by MCT, and destabilizing the

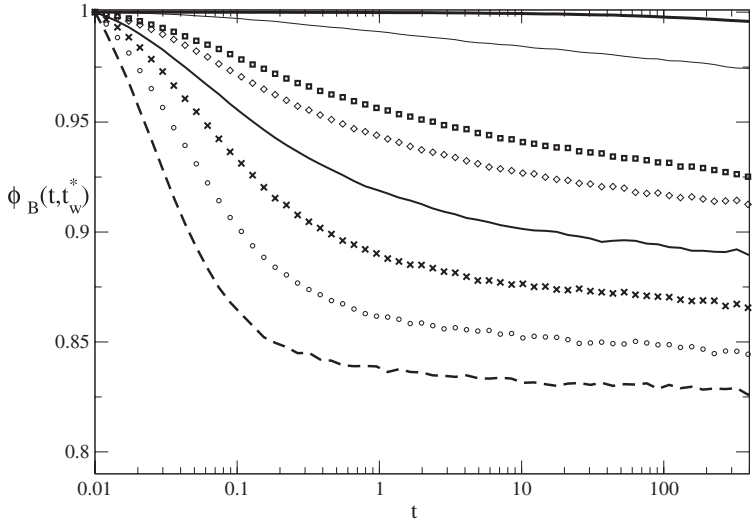

Figure 5. Time evolution of the bond correlators $\phi_B\,(t_w + t,\, t_w)$ for $\phi = 0.635$ and t_w^*. Temperatures are the same as in the previous figure (corresponding to the same symbols).

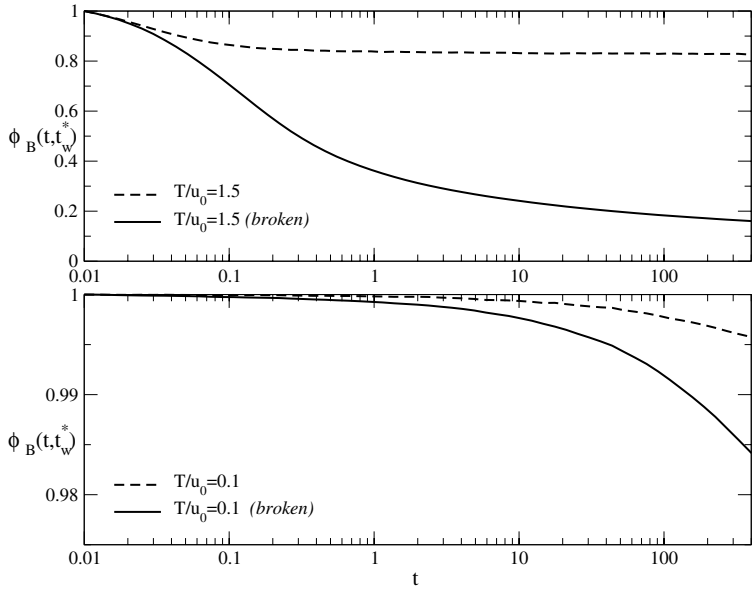

Figure 6. Time evolution of the bond correlators $\phi_B\,(t_w+t,\, t_w)$ for $\phi = 0.635$ and t_w^* for temperatures $T/u_0 = 1.5$ and 0.1, comparing the case when bonds after being broken are still counted (same as 5, dashed curves) or not (curves labelled as 'broken', full curves).

attractive glass. The study of the effect of the bond lifetime on the full dynamical behaviour of short-ranged attractive colloids has also been explored in [31].

In the present work, we support the hypothesis of bond-breaking hopping processes pre-empting the observation of a sharp glass–glass transition, as predicted by MCT, showing that results for the density correlators as shown in figure 4 do not depend on the chosen waiting time or on the history path dependence.

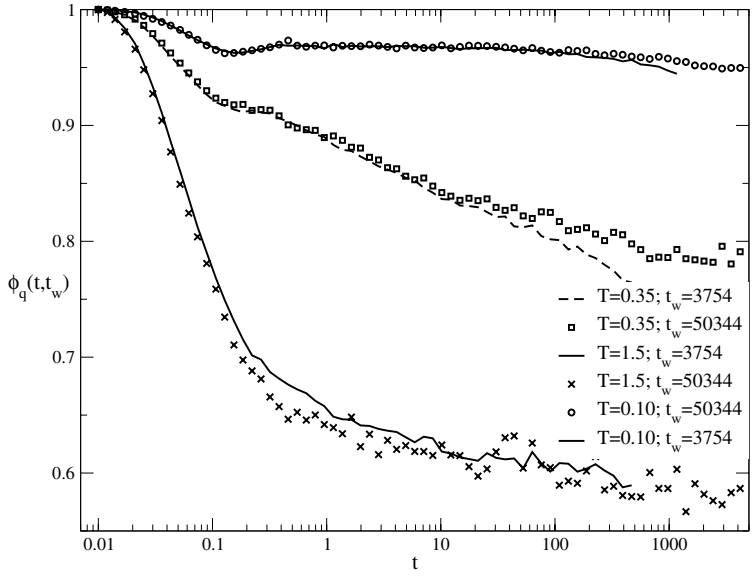

Figure 7. Study of the waiting time dependence for three different temperatures at $\phi = 0.635$. Points refer to $t_w = 50\,344$, one order of magnitude larger than t_w^*. Clearly, the plateaux are not affected by the difference in waiting time, at any temperature.

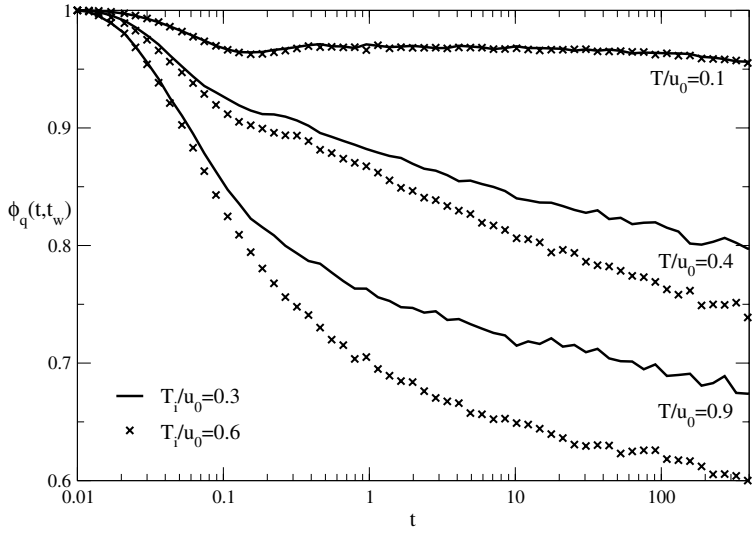

Figure 8. Study of the history dependence for three different temperatures at $\phi = 0.635$ and t_w^*. Points refer to initial state point B in figure 2, while solid lines are for the standard initial state point A.

Thereby, we first report in figure 7 the density correlation functions for three representative temperatures, i.e. $T = 1.5$, 0.35, and 0.1, for a waiting time of 5×10^4, compared to the case examined so far for a t_w smaller by a full order of magnitude. These results are averaged over up to 40 configurations only, due to the very large computer time involved in the calculation (approximately 10^3 CPU hours for each temperature). It is evident that no significant change

in the density correlator behaviour arises, though small discrepancies are also present due to the larger errors present in the longer simulation runs. However, the most important feature to underline is that an increase in waiting time is not manifest in an increase of the time duration of the attractive plateau. Our study shows that the stability of such a plateau, i.e. of the bond lifetime, can only be achieved by decreasing temperature. Thus, the observed phenomenon is entirely due to bond dynamics, which is independent of the waiting time and completely controls the attractive glass transition.

Of course, an interesting issue would be to know exactly where, at infinite times, the attractive glass correlation functions would decay to. In other words, we know that the plateau must be finite, and its lower bound should be represented by the hard-sphere plateau. So, we can speculate that the long-time cage of the attractive glass is still of the order of the hard-sphere one, though at each time particles are trapped within the attractive well-width, which is highly affected by breaking processes, in contrast to simple packing. Unfortunately, we cannot support this picture by simulations, since it would require many additional decades in time, beyond computational efforts.

The last point we wish to address is the dependence on the chosen liquid initial state. Indeed, one might argue that we started our non-equilibrium (compression + quenching) path from a state point close to a hard-sphere glass. Thus, we can repeat the full procedure from a different initial state close to the attractive glass transition. For this purpose, we refer to the initial state point B of figure 2. Results for the density correlators are compared, for the two different initial points, in figure 8, for temperatures $T/u_0 = 0.1$, 0.4, and 0.9. It is clear that quantitatively results are different, but qualitatively they are not. As expected, starting from a lower temperature causes the produced glass to have a higher correlation function, i.e. it imprints in it more of the attractive features. However, after the microscopic time, the decay is very similar in the two cases. Most importantly, the lowest temperature plateau is not stabilized by the different path.

It is interesting to note that if one examines the complete T-dependence of the density correlators at the same isochore $\phi = 0.625$ as in figure 4, but now starting from B, one does not observe the same non-monotonic behaviour, at high temperatures, for the density correlators. This is due to the fact that we are starting from a configuration close to the attractive line, which somehow remains imprinted in the *memory* of the system (see figures 8, 9). Thus, probably, our small time window of observation is not sufficient for the system to forget about its initial state, which prevents the observation of smaller plateaux especially at higher temperatures. In other words, the system cannot really feel enough competition from two transitions, and the only relevant one for the dynamics here is the glass–glass one. Interestingly enough, this behaviour resembles closely the one at the highest isochore ($\phi = 0.635$) starting from A [29].

Finally, we want to focus on the behaviour of the static structure factors in the glassy region. As explained above, $S(q)$ is the input needed to solve MCT equations, and at the glass–glass transition it does not have any peculiar change, other than the smooth one characteristic of a slight change of thermodynamic control parameters. In figure 9, we show the (total) static structure factors for $T/u_0 = 0.1$ and 0.9 together with the equilibrium configuration one, both for the path starting from point A (top panel) and from point B (bottom panel). It is clear that the structure just changes smoothly along the quenching paths, but does change with respect to the initial equilibrium state because of the density increase. In the glass, no detectable waiting time dependence for the structure is observed. Static structure factors between the two panels, corresponding to the same temperatures after different paths, cannot be really distinguished within numerical errors. However, we expect small changes due to the different imprinted structures for the initial state-point. This could help to explain why the results for the dynamical correlators are different between the two paths (see figure 8). The results shown

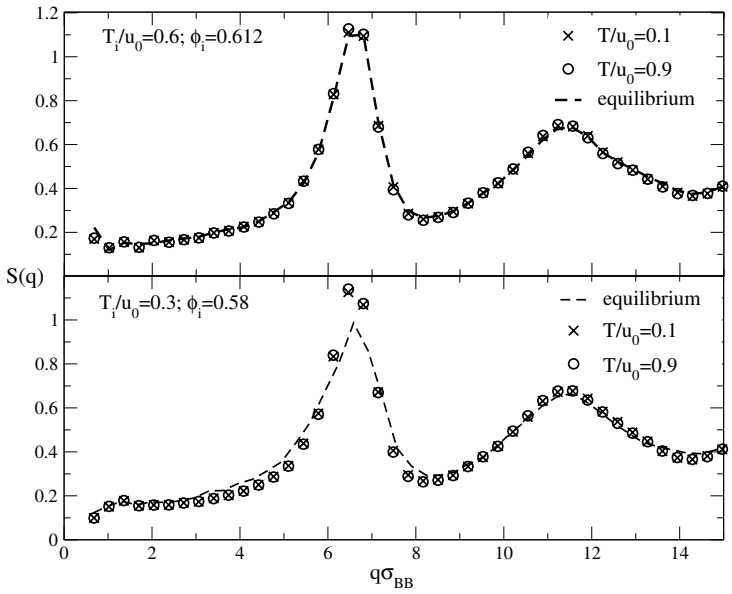

Figure 9. Static structure factors at different temperatures for $\phi = 0.635$, compared to each other and to the equilibrium static structure factor of the initial liquid: the top panel is for initial state point A ($T_i = 0.6$, $\phi_i = 0.612$), the bottom for initial state point B ($T_i = 0.3$, $\phi_i = 0.58$).

here for the static structure factors are quite different than those found in a micellar system [11], and that could explain the different conclusions drawn in that paper.

4. Conclusions

In this paper, we have reported numerical simulations along the theoretically predicted glass–glass transition between repulsive and attractive glass for a simple model of short-ranged attractive colloids. A simple mapping between theory and simulations, performed for this particular model, allowed us to have an accurate location of this glass–glass transition, and thus to have a consistent test of the theoretical predictions by simulations in the glass.

Studying the glassy dynamics, we can discriminate time intervals where waiting time does not play a significant role, and where there is only a minor dependence on the preparation of the glassy state. It is, therefore, an ideal system to study and compare the two mechanisms of glassification, i.e. packing and attraction.

Our results clearly show that a glass–glass transition exists. Indeed, there is a significant difference in the dynamical behaviour between hard-sphere and attractive glass, though the crossover from one kind to the other is smoother than predicted by MCT. Thus, the transition is not manifest as sharply as predicted by the theory, due to bond-breaking processes that reduce the stability of the attractive glass. The detailed studies of waiting time and path dependence strengthen this interpretation, because they do not have any effect on the stability of the attractive plateau. This, indeed, can only be made longer lasting by a decrease of temperature, i.e. an (Arrhenius) increase of the bond lifetime. Therefore, we claim that bond-breaking activated processes have the same relevance in attractive glass as they do in molecular glass-formers, while hard-sphere glasses, due to their entropic origin, are basically unaffected by them. On the other hand, the intrinsically different natures of the two glasses can still be experimentally detected. In particular, for systems where the bond lifetime is long enough,

or equivalently by looking at timescales that are shorter than the bond lifetime, the MCT predictions for the glass–glass transition could be fully recovered.

Acknowledgments

We acknowledge support from MIUR COFIN 2002, FIRB and INFM Iniziativa Calcolo Parallelo. We thank S Buldyrev for the MD Code and W Götze, M Fuchs, W Poon and E Bartsch for discussions.

References

[1] Fabbian L, Götze W, Sciortino F, Tartaglia P and Thiery F 1999 *Phys. Rev.* E **59** R1347
Fabbian L, Götze W, Sciortino F, Tartaglia P and Thiery F 1999 *Phys. Rev.* E **60** 2430
[2] Bergenholtz J and Fuchs M 1999 *Phys. Rev.* E **59** 5706
[3] Dawson K A, Foffi G, Fuchs M, Götze W, Sciortino F, Sperl M, Tartaglia P, Voigtmann Th and Zaccarelli E 2001 *Phys. Rev.* E **63** 011401
[4] Zaccarelli E, Foffi G, Tartaglia P, Sciortino F and Dawson K A 2001 *Phys. Rev.* E **63** 031501
[5] Dawson K A, Foffi G, Sciortino F, Tartaglia P and Zaccarelli E 2001 *J. Phys.: Condens. Matter* **13** 9113
[6] Dawson K A, Foffi G, McCullagh G D, Sciortino F, Tartaglia P and Zaccarelli E 2002 *J. Phys.: Condens. Matter* **14** 2223
[7] Götze W and Sperl M 2003 *J. Phys.: Condens. Matter* **15** S869
[8] Mallamace F, Gambadauro P, Micali N, Tartaglia P, Liao C and Chen S H 2000 *Phys. Rev. Lett.* **84** 5431
[9] Pham K N, Puertas A M, Bergenholtz J, Egelhaaf S U, Moussaid A, Pusey P N, Schofield A B, Cates M E, Fuchs M and Poon W C K 2002 *Science* **296** 104
[10] Eckert T and Bartsch E 2002 *Phys. Rev. Lett.* **89** 125701
Eckert T and Bartsch E 2003 *Faraday Discuss.* **123** 51
[11] Chen W R, Chen S H and Mallamace F 2002 *Phys. Rev.* E **66** 021403
Chen S H, Chen W R and Mallamace F 2003 *Science* **300** 619
[12] Grandjean J and Mourchid A 2004 *Europhys. Lett.* **65** 712
[13] Puertas A M, Fuchs M and Cates M E 2002 *Phys. Rev. Lett.* **88** 098301
Puertas A M, Fuchs M and Cates M E 2003 *Phys. Rev.* E **67** 031406
[14] Foffi G, Dawson K A, Buldyrev S, Sciortino F, Zaccarelli E and Tartaglia P 2002 *Phys. Rev.* E **65** 050802
[15] Zaccarelli E, Foffi G, Dawson K A, Buldyrev S, Sciortino F and Tartaglia P 2002 *Phys. Rev.* E **66** 041402
[16] Sciortino F, Tartaglia P and Zaccarelli E 2003 *Phys. Rev. Lett.* **91** 268301
[17] Zaccarelli E, Buldyrev S, Sciortino F and Tartaglia P 2004 *Physica* A at press
(Zaccarelli E, Buldyrev S, Sciortino F and Tartaglia P 2003 *Preprint* cond-mat/0310765)
[18] Zaccarelli E, Löwen H, Wessels P P F, Sciortino F, Tartaglia P and Likos C N 2004 *Phys. Rev. Lett.* **92** 225703
(Zaccarelli E, Löwen H, Wessels P P F, Sciortino F, Tartaglia P and Likos C N 2004 *Preprint* condmat/0402254)
[19] Sciortino F 2002 *Nat. Mater.* **1** 145
[20] Götze W and Sperl M 2002 *Phys. Rev.* E **66** 011405
[21] Götze W 1991 *Liquids, Freezing and Glass Transition* ed J P Hansen, D Levesque and J Zinn-Justin (Amsterdam: North-Holland) p 287
[22] Götze W 1999 *J. Phys.: Condens. Matter* **11** A1
[23] Das S P and Mazenko G F 1986 *Phys. Rev.* A **34** 2265
Götze W and Sjögren L 1987 *Z. Phys.* B **65** 415
[24] Angelani L, Di Leonardo R, Ruocco G, Scala A and Sciortino F 2000 *Phys. Rev. Lett.* **85** 5356
Grigera T S, Cavagna A, Giardina I and Parisi G 2002 *Phys. Rev. Lett.* **88** 055502
[25] Kob W and Barrat J-L 1997 *Phys. Rev. Lett.* **78** 4581
Cugliandolo L F 2002 *Preprint* cond-mat/0210312
[26] Sciortino F and Tartaglia P 2001 *J. Phys.: Condens. Matter* **13** 9127
[27] Sperl M 2003 *Phys. Rev.* E **68** 031405
[28] We have shown that Percus–Yevick approximation is very accurate in the reentrant liquid region in Zaccarelli E, Foffi G, Dawson K A, Buldyrev S, Sciortino F and Tartaglia P 2003 *J. Phys.: Condens. Matter* **15** 223
[29] Zaccarelli E, Foffi G, Sciortino F and Tartaglia P 2003 *Phys. Rev. Lett.* **91** 108301
[30] Foffi G, Götze W, Sciortino F, Tartaglia P and Voigtmann T 2004 *Phys. Rev.* E **69** 011505
[31] Saika-Voivod I, Zaccarelli E, Sciortino F and Tartaglia P 2004 *Phys. Rev.* E submitted